Article

Cooperation between Artificial Receptors and Supramolecular Hydrogels for Sensing and Discriminating Phosphate Derivatives

Satoshi Yamaguchi, Ibuki Yoshimura, Takahiro Kohira, Shun-ichi Tamaru, and Itaru Hamachi

J. Am. Chem. Soc., **2005**, 127 (33), 11835-11841• DOI: 10.1021/ja052838y • Publication Date (Web): 30 July 2005

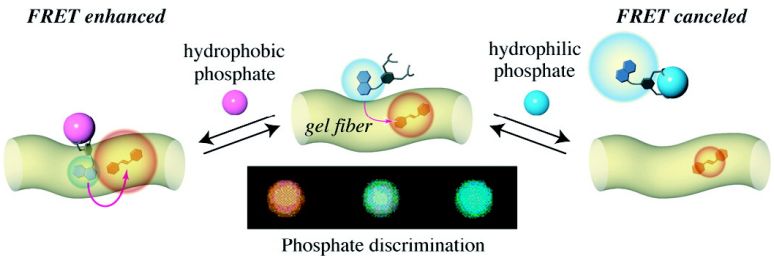

More About This Article

Additional resources and features associated with this article are available within the HTML version:

- Supporting Information
- Links to the 19 articles that cite this article, as of the time of this article download
- Access to high resolution figures
- Links to articles and content related to this article
- Copyright permission to reproduce figures and/or text from this article

View the Full Text HTML

J|A|C|S
ARTICLES
Published on Web 07/30/2005

Cooperation between Artificial Receptors and Supramolecular Hydrogels for Sensing and Discriminating Phosphate Derivatives

Satoshi Yamaguchi, Ibuki Yoshimura, Takahiro Kohira, Shun-ichi Tamaru, and Itaru Hamachi*

Contribution from PRESTO (Synthesis and Control, Japan Science and Technology), Department of Synthetic Chemistry and Biological Chemistry, Kyoto University, Katsura, Nishikyo-ku, Kyoto 615-8510, Japan

Received May 2, 2005; E-mail: ihamachi@sbchem.kyoto-u.ac.jp

Abstract: This study has successfully demonstrated that the cooperative action of artificial receptors with semi-wet supramolecular hydrogels may produce a unique and efficient molecular recognition device not only for the simple sensing of phosphate derivatives, but also for discriminating among phosphate derivatives. We directly observed by confocal laser scanning microscopy that fluorescent artificial receptors can dynamically change the location between the aqueous cavity and the hydrophobic fibers upon guest-binding under semi-wet conditions provided by the supramolecular hydrogel. On the basis of such a guest-dependent dynamic redistribution of the receptor molecules, a sophisticated means for molecular recognition of phosphate derivatives can be rationally designed in the hydrogel matrix. That is, the elaborate utilization of the hydrophobic fibrous domains, as well as the water-rich hydrophilic cavities, enables us to establish three distinct signal transduction modes for phosphate sensing: the use of (i) a photoinduced electron transfer type of chemosensor, (ii) an environmentally sensitive probe, and (iii) an artificial receptor displaying a fluorescence resonance energy transfer type of fluorescent signal change. Thus, one can selectively sense and discriminate the various phosphate derivatives, such as phosphate, phospho-tyrosine, phenyl phosphate, and adenosine triphosphate, using a fluorescence wavelength shift and a seesaw type of ratiometric fluorescence change, as well as a simple fluorescence intensity change. It is also shown that an array of the miniaturized hydrogel is promising for the rapid and high-throughput sensing of these phosphate derivatives.

Introduction

Chemosensors are expected to be powerful molecular tools for the analysis of many target molecules, such as biological markers, environmental pollutants, and others.[1] Among them, chemosensors that can work under aqueous conditions are especially valuable for detecting substances of biological significance, because many biomarkers are soluble only in aqueous solution.[2] When one designs an efficient chemosensor for a specific target in aqueous systems, there are generally still two major difficulties: developing an excellent binding motif toward the target molecule, and equipping the receptor with a signal read-out device. Since the concurrent solution of these two matters is often difficult, an efficient artificial receptor does not necessarily become a good sensor, and vice versa. Phosphate anion sensors that can work in aqueous solution,[3] for example, have not been well developed for these reasons, and in particular, discrimination among the phosphate anions family, such as phosphate, phosphate esters, adenosine triphosphate (ATP) derivatives, etc., is still very difficult.

In addition, a means of rapid and high-throughput sensing using chemosensors has been highly desired for various analytes in recent years.[4] Although such an achievement is expected to significantly extend the application of chemosensors, there are several problems to be overcome for this to be accomplished. The effective immobilization of sensor molecules on a solid support is regarded to be primarily important in order to carry

(1) (a) Cooke, G.; Rottello, V. M. *Chem. Soc. Rev.* **2002**, *31*, 275. (b) Rebek, J., Jr. *Chem. Commun.* **2000**, 637. (c) Peezuh, M. W.; Hamilton, A. D. *Chem. Soc. Rev.* **2000**, *100*, 2479.

(2) (a) Nakata, E.; Nagase, T.; Shinkai, S.; Hamachi, I. *J. Am. Chem. Soc.* **2004**, *126*, 490. (b) Nagase, T.; Nakata, E.; Shinkai, S.; Hamachi, I. *Chem.—Eur. J.* **2003**, *9*, 3660. (c) Nagase, T.; Shinkai, S.; Hamachi, I. *Chem. Commun.* **2001**, 229. (d) Hamachi, I.; Nagase, T.; Shinkai, S. *J. Am. Chem. Soc.* **2000**, *122*, 12065. (e) James, T. D.; Shinkai, S. *Host—Guest Chemistry*; Topics in Current Chemistry 218; Springer-Verlag: Berlin, 2002; pp 159—200. (f) Piatek, A. M.; Bomble, Y. J.; Wiskur, S. L.; Anslyn, E. V. *J. Am. Chem. Soc.* **2004**, *126*, 6072. (g) Rekharsky, M.; Inoue, Y.; Tobey, S.; Metzger, A.; Anslyn, E. *J. Am. Chem. Soc.* **2002**, *124*, 14959. (h) McCleskey, S. C.; Metxger, A.; Simmons, C. S., Anslyn, E. V. *Tetrahedron* **2002**, *58*, 621. (i) Disney, M. D.; Zheng, J.; Swager, T. M.; Seeberger, P. H. *J. Am. Chem. Soc.* **2004**, *126*, 13343.

(3) (a) Ojida, A.; Mito-oka, Y.; Sada, K.; Hamachi, I. *J. Am. Chem. Soc.* **2004**, *126*, 2454. (b) Ojida, A.; Mito-oka, Y.; Inoue, M.; Hamachi, I. *J. Am. Chem. Soc.* **2002**, *124*, 6256. (c) Abe, H.; Mawatari, Y.; Teraoka, H.; Fujimoto, K.; Inouye, M. *J. Org. Chem.* **2004**, *69*, 495. (d) Aoki, S.; Kimura, E. *Rev. Mol. Biotechnol.* **2002**, *90*, 129. (e) Lee, D. H.; Im, J. H.; Son, S. U.; Chung, Y. K.; Hong, J.-I. *J. Am. Chem. Soc.* **2003**, *125*, 7752. (f) Tobey, S. L.; Jones, B. D.; Anslyn, E. V. *J. Am. Chem. Soc.* **2003**, *125*, 4026. (g) Han, M. S.; Kim, D. H. *Angew. Chem., Int. Ed.* **2002**, *41*, 3809. (h) Mizukami, S.; Nagano, T.; Urano, Y.; Odani, A.; Kikuchi, K. *J. Am. Chem. Soc.* **2002**, *124*, 3920. (i) Sebo, L.; Diedetich, F. *Helv. Chem. Acta* **2000**, *83*, 93. (j) Vance, D. H.; Czarnik, A. W. *J. Am. Chem. Soc.* **1994**, *116*, 9397. (k) Hosseini, M. W.; Blacker, A. J.; Lehn, J.-M. *J. Am. Chem. Soc.* **1990**, *112*, 3896.

out convenient and high-throughput sensing.[5] As a conventional method, the covalent fixation of sensors on polymers or glass substrates has been widely used. However, several drawbacks should be improved upon, such as the suppression of the binding and/or sensing ability induced by the immobilization relative to the original one displayed in a homogeneous solution, the required introduction of an attachment site to the sensor molecules, etc. We recently examined molecular recognition in a supramolecular hydrogel using fluorescent probes and indicated that these chemosensors are noncovalently immobilized in a water-rich environment while practically retaining the original binding functions.[6] This supramolecular entrapment by the hydrogel may be a unique and alternative method for the fixation of chemosensors.

We successfully demonstrate herein the dynamic redistribution of the receptor molecule upon guest-binding between the aqueous microcavity and the hydrophobic nanofibers, both of which are formed by the supramolecular hydrogel. On the basis of such a unique feature, it is clear that the supramolecular hydrogel can play a more active role in the molecular recognition events than simply being the immobilization matrix; that is, there is a cooperative action between the artificial receptors and the hydrogel matrix not only to sense the phosphate anion derivatives, but to also discriminate the phosphate anion family from each other on the basis of the pattern of the fluorescence intensity change and wavelength shift of the artificial receptors entrapped in the supramolecular hydrogel. We also show that an array of the down-sized hydrogel including these chemosensors is promising for the rapid and simple sensing of phosphate derivatives which can be distinguished by the naked eye or a digital camera.

Results and Discussion

Phosphate Derivatives Sensing by a PET-Type Fluorescent Chemosensor Embedded in Supramolecular Hydrogel. As a gel matrix, we employed a glycosylated amino acetate type of hydrogelator **1** (Chart 1), the hydrogel of which includes many nano-sized fibers bearing continuously well-developed hydrophobic domains and many micro-sized cavities that should be filled with immobilized water in the semi-wet hydrogel state as reported previously.[4f,6]

To evaluate the function of an artificial receptor entrapped in a supramolecular hydrogel matrix, we initially conducted a fluorescent binding assay using a fluorescent chemosensor for the phosphate anion and its derivatives. Figure 1a shows a fluorescence change of bis-Zn/Dpa-anthracene **2**[3a] embedded in a transparent hydrogel **1** with the addition of ATP. Upon the

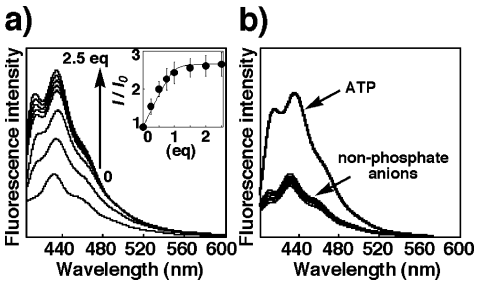

Figure 1. (a) Fluorescence spectral change (measured by MCPD) of the bis-Zn/Dpa-anthracene **2** (20 μM) embedded in the hydrogel **1** upon addition of ATP: [ATP] = 0−50 μM at λ_{ex} = 380 nm. (b) Addition of non-phosphate anions (sulfate, nitrate, acetate, azide, bromide, chloride, fluoride) did not cause any fluorescence change: [**2**] = 40 μM, [anion] = 200 μM at λ_{ex} = 380 nm.

Chart 1. Chemical Structures

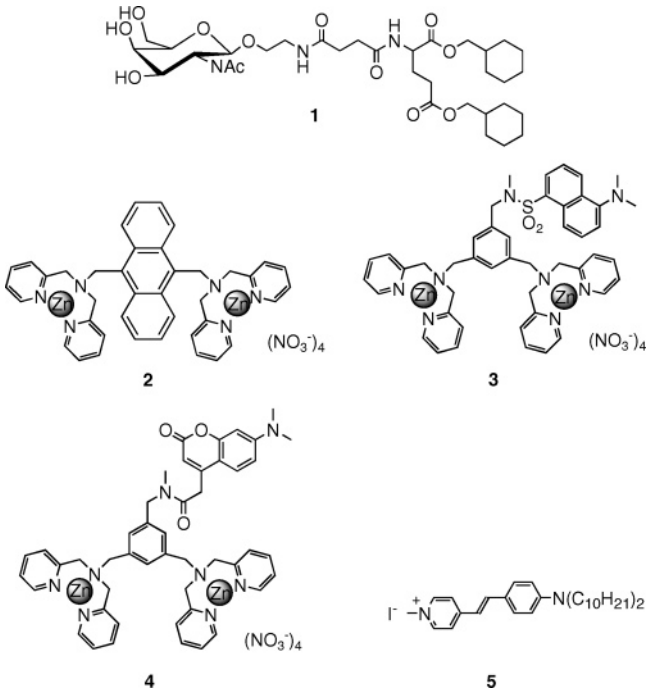

ATP addition, an emission at 435 nm increased by 2.6-fold in fluorescence intensity, which enables us to monitor the binding event because of the photoinduced electron transfer (PET) type of sensing mechanism. This spectral change is identical to that observed in aqueous solution. The fluorescence titration curve obeyed a typical saturation pattern which produced a binding constant greater than 10^6 M^{-1}, which is larger than those for phosphate (2.3×10^5 M^{-1}), phenyl phosphate (PhP, 5.4×10^4 M^{-1}), and phospho-tyrosine (phospho-Tyr, 7.4×10^4 M^{-1}) determined previously by us.[6] In contrast, the addition of non-phosphate anions, such as sulfate, nitrate, acetate, azide, halide, etc., did not cause any fluorescence change (Figure 1b), indicating that such a selectivity of **2** embedded in the hydrogel agrees well with the selectivity of **2** in aqueous solution. Therefore, it is concluded that the semi-wet microcavity produced by the hydrogel network is suitable for immobilizing artificial fluorescent chemosenors while retaining their original function.

Use of Hydrophobic Microdomain of Supramolecular Hydrogel Fiber for Discrimination of Phosphate Derivatives. The previous section indicates that the receptor **2** can distinguish

(4) (a) Lavinge, J. J.; Anslyn, E. V. *Angew. Chem., Int. Ed.* **2001**, *40*, 3118. (b) Heath, R. E.; Dykes, G. M.; Fish, H.; Smith, D. K. *Chem.−Eur. J.* **2003**, *9*, 850. (c) The chipping forecast. *Nature Genet. (Suppl.)* **1999**, *21*, 1−60. (d) Yang, Z.; Xu, B. *Chem. Commun.* **2004**, *21*, 2424−2425. (e) Yang, Z.; Gu, H.; Fu, D.; Gao, P.; Lam, J. K.; Xu, B. *Adv. Mater.* **2004**, *16*, 1440. (f) Kiyonaka, S.; Sada, K.; Yoshimura, I.; Shinkai, S.; Kato, N.; Hamachi, I. *Nat. Mater.* **2004**, *3*, 58. (g) Tamaru, S.-I.; Yamaguchi, S.; Hamachi, I. *Chem. Lett.* **2005**, 294. (h) Seong, S.-Y.; Choi, C.-Y. *Proteomics* **2003**, *3*, 2176.

(5) (a) Daniel, M.-C.; Astruc, D. *Chem. Rev.* **2004**, *104*, 293. (b) Verma, A.; Nakade, H.; Simard, J. M.; Rotello, V. M. *J. Am. Chem. Soc.* **2004**, *126*, 10806. (c) Shenhar, R.; Rotello, V. M. *Acc. Chem. Res.* **2003**, *36*, 549. (d) Mulder, A.; Auletta, T.; Sartori, A.; Del Ciotto, S.; Casnati, A.; Ungaro, R.; Huskens, J.; Reinhoudt, D. N. *J. Am. Chem. Soc.* **2004**, *126*, 6627. (e) Raymo, F. M.; Cejas, M. A. *Org. Lett.* **2002**, *4*, 3183. (f) Otsuka, H.; Akiyama, Y.; Nagasaki, Y.; Kataoka, K. *J. Am. Chem. Soc.* **2001**, *123*, 8226.

(6) Yoshimura, I.; Miyahara, Y.; Kasagi, N.; Yamane, H.; Ojida, A.: Hamachi, I. *J. Am. Chem. Soc.* **2004**, *126*, 12204.

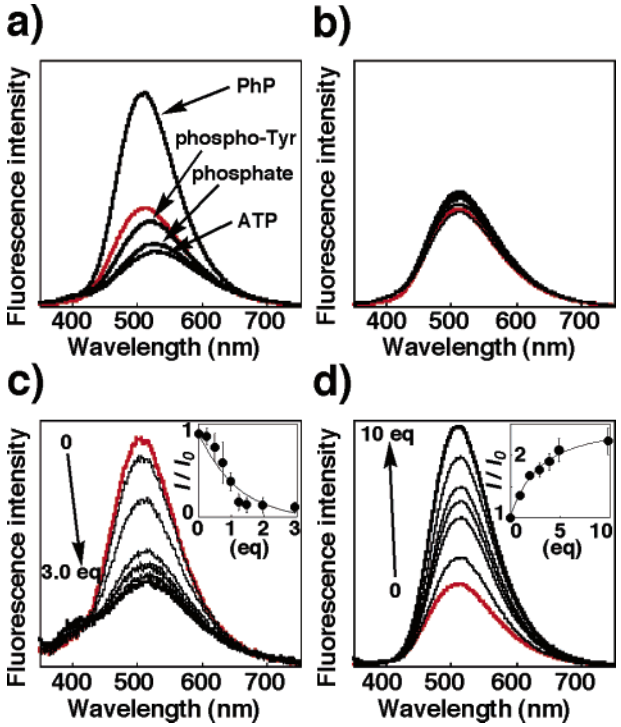

Figure 2. Three patterns of change observed in the fluorescence spectra of the hydrogel **1** containing the dansyl-appended receptor **3**. (a) Fluorescence spectral change of **3** (60 μM, red line) embedded in **1** upon addition of PhP, ATP, phosphate, or phospho-Tyr. The emission intensity of **3** increases with the blue-shift for PhP, whereas the intensity decreases with the red-shift for ATP, phosphate, or pyospho-Tyr. (b) Fluorescence spectra in the presence of other non-phosphate anions: [anion] = 600 μM at λ_{ex} = 322 nm. (c,d) Fluorescence spectral change and the fluorescence titration plots (inset) of **3** embedded in **1** upon addition of ATP or PhP, respectively: [**3**] = 20 μM, [ATP] = 0−60 μM (c), [**3**] = 60 μM, [PhP] = 0−600 μM (d) at λ_{ex} = 322 nm.

phosphate anion derivatives from other anionic species on the basis of fluorescence, but it cannot discriminate a specific phosphate species among the phosphate family. It is expected that the effective utilization of the hydrophobic nanofiber domain in the supramolecular hydrogel may allow a more selective discrimination among the phosphate derivatives. For this study, another phosphate receptor **3** was synthesized and employed, which has two Zn/Dpa sites like the chemosensor **2** and is attached to an environmentally sensitive fluorophore (dansyl).[7] After the receptor **3** was immobilized in the supramolecular hydrogel, various anions including phosphate derivatives were added. As shown in Figure 2a,b, there are roughly three patterns of change observed in the fluorescence spectra. That is, the emission intensity of **3** (at 512 nm) increases with the emission blue-shift for PhP, and the intensity decreases with the red-shift of the emission for ATP, phosphate, and phospho-Tyr, whereas it never changes for non-phosphate anions. Figure 2c shows the fluorescence change in the detailed titration experiment. Clearly, the emission gradually decreased (I/I_0 = 0.56) with the concurrent red-shift of the emission maximum (528 nm) upon addition of ATP. In contrast, a reverse type of spectral change occurred when PhP (I/I_0 = 2.1, 503 nm), which is a more hydrophobic phosphate derivative than ATP, was added to the hydrogel spot containing the chemosensor **3** (shown in Figure 2d). These spectral changes obeyed a typical saturation curve, yielding binding constants of 1.8 × 10^5 M^{-1} for ATP and 7.2 × 10^3 M^{-1} for PhP. These values are slightly reduced relative to the values determined by the PET type of chemosensor **2**, which may be due to the additional guest redistribution process involved in sensing. For phospho-Tyr (523 nm, I/I_0 = 0.87) and phosphate (527 nm, I/I_0 = 0.64), an intermediate range of change was observed in the fluorescence. This result indicates that the phosphate anion species may be discriminated from each other by using both the intensity change and the wavelength shift.

(7) Stryer, L. *J. Mol. Biol.* **1965**, *13*, 482−495.

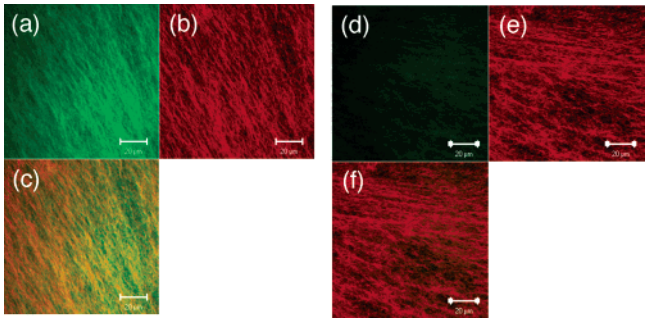

Figure 3. Confocal laser scanning micrographs of the rhodamine-stained hydrogels containing the dansyl-appended receptor **3** in the presence of PhP (a−c), or **3** in the presence of ATP (d−f). The fluorescence image of the localization of the receptor **3** (the excitation wavelength at 351 nm, green color) is shown in panels a and d, and the image of the rhodamine-stained gel fiber (the excitation wavelength at 543 nm, red color) is shown in panels b and e. The merged images (c, f) were obtained by summing the images a and b, or d and e, respectively. These images were obtained 30 min after phosphate solutions were dropped onto hydrogel spots.

It is important to note that such a fluorescence change does not occur in aqueous solution nor in the case of agarose gel, a polymer-based hydrogel having no hydrophobic domains (see Supporting Information Figure S1), indicating that the hydrophobic domain of the present supramolecular hydrogel should be crucial for the guest-induced fluorescence change. In addition, it seemed that the fluorescence response was closely associated with the hydrophilicity of the guest molecules; that is, the strongly hydrophilic ATP induced a red-shift in the emission of **3** with the reduced intensity, whereas the rather hydrophobic PhP caused the emission increase with the blue-shift. These spectral changes imply that the microenvironment of the **3**/ATP complex should be more hydrophilic than that of **3** itself, whereas the **3**/PhP complex should locate in the more hydrophobic microenvironment relative to the original receptor **3**. This suggests that the artificial receptor **3** is sufficiently mobile in this supramolecular hydrogel matrix and the localization is altered between the hydrophilic aqueous cavity and the hydrophobic fibrous domain upon guest-binding.

Direct Observation of the Spatial Redistribution of Artificial Receptor Using Confocal Laser Scanning Microscopy. Direct evidence for the guest-binding induced spatial redistribution of the receptor **3** was provided by confocal laser scanning microscopy (CLSM). Figure 3 shows typical CLSM images of the supramolecular hydrogel containing **3** in the presence of the guest. For fluorescently staining the gel fiber, a hydrophobic rhodamine probe bearing a long alkyl chain was used (Figure 3b,e). For the PhP addition, the hydrogel fibers were also stained with the green fluorescence due to the dansyl fluorophore (Figure 3a). This is perfectly overlapped with the fiber shape obtained by the rhodamine staining, and thus, the merged image in Figure 3c produced the yellow-colored fibers by mixing the red (rhodamine) and green (dansyl) colors. This

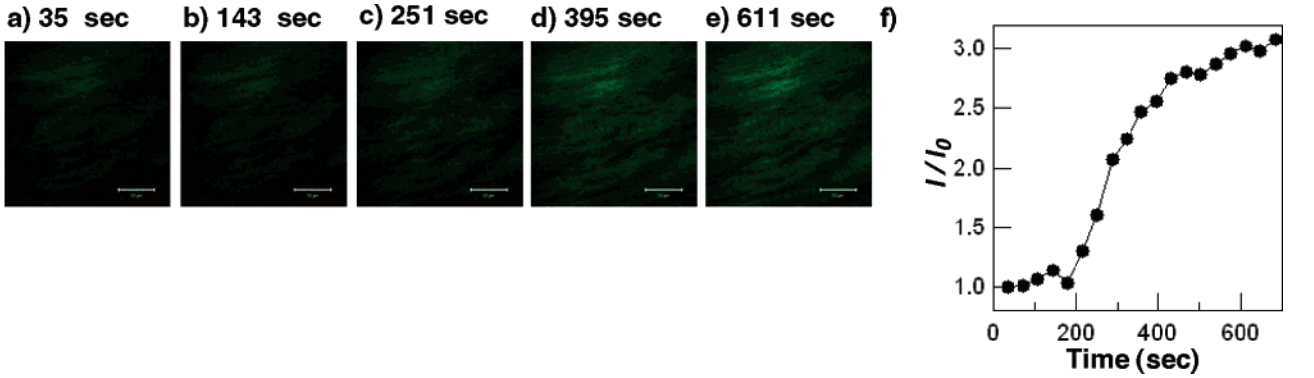

Figure 4. Time-dependent confocal laser scanning micrographs of the hydrogel **1** containing the dansyl-appended receptor **3** after the PhP addition (a−e), where the time is given in seconds. The time course of the emission intensity change in a localized spot of **1** was plotted in panel f.

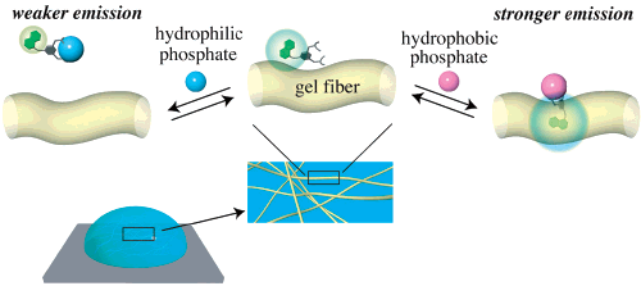

Figure 5. Schematic illustration of the chemosensor redistribution upon the binding to a hydrophobic or hydrophilic phosphate derivative between the hydrophobic hydrogel nanofiber and the hydrophilic cavity.

result indicates that the dansyl-appended **3** was co-localized with the rhodamine dye along the hydrophobic fibrous domain produced by the supramolecular hydrogel **1**. In contrast, in the presence of ATP, such a yellow color was not produced by merging (Figure 3f) the image of the rhodamin-stained hydrogel (Figure 3e) with that of the dansyl-appended receptor (Figure 3d), but instead, the simple coincidence of Figure 3f with Figure 3e was produced, indicating that the receptor **3** was not spatially co-localized with the rhodamine-stained gel fibers in the case of ATP. Consequently, the rather dark image appeared in Figure 3d, suggesting that the receptor **3** was not distributed to the fiber domain, but dispersed in the aqueous space of the hydrogel.

The time trace experiment using CLSM strongly supported the above discussion. Before the PhP addition, the CLSM view was rather dark and only the weak emission was smeared, but many brighter fibers gradually appeared after the PhP addition (Figure 4a−e). The emission intensity of a fiber domain increases after about a 200 s induction period and saturates at 600 s (Figure 4f). These CLSM images may be explained by the fact (Figure 5) that the receptor **3** is almost uniformly dispersed in the hydrogel before the host−guest interaction, and upon the PhP binding it is accumulated in the hydrophobic domain of the supramolecular nanofiber in the semi-wet hydrogel. Because the nanofiber region is rather hydrophobic, the stronger emission of the dansyl moiety of **3** was reasonably observed. On the other hand, the CLSM image after ATP addition did not drastically change, and the intensity was slightly lessened relative to that at the initial stage (data not shown).

These results clearly indicate that the receptor **3** can alter the localization in the semi-wet supramolecular hydrogel, depending on the guest-binding. More importantly, the nanofiber can be used as a unique domain to monitor a molecular recognition process, so that the receptor **3** can not only selectively sense the phosphate derivatives, but also discriminate the structural variety of these derivatives on the basis of the pattern of the fluorescence intensity and the wavelength shift.

Construction of FRET Type of Sensing System and a Semi-wet Molecular Recognition Chip. The guest-dependent redistribution of the artificial receptor may be extended to the rational construction of a fluorescence resonance energy transfer (FRET)[8] type of read-out system in the semi-wet supramolecular hydrogel. By juxtaposition of an additional fluorophore in the hydrophobic domain of the nanofiber, an energy transfer should take place between the fluorescent receptor and the added fluorophore. Since the FRET efficiency is significantly dependent on the distance between the two fluorophores, the receptor redistribution upon guest-binding should alter the distance so as to cause a seesaw type of fluorescence change.

As a suitable FRET pair, a coumarin-appended receptor **4** for phosphate derivatives and a hydrophobic styryl dye **5** (Supporting Information Figure S2), as a FRET donor and an acceptor, respectively, were embedded in the supramolecular hydrogel. Figure 6a,b shows the fluorescence spectral changes in the titration with PhP and ATP, respectively. Before the addition of PhP, two emission peaks at 485 and 569 nm due to the coumarin and the styryl dye, respectively, appeared with almost the same intensity ($I_{569}/I_{485} = 1.1$). With the increase in PhP, the peak at 485 nm gradually decreased with a slight blue-shift and the peak at 569 nm was concurrently intensified, so that the ratio of I_{569}/I_{485} increased to 2.5. This seesaw type of spectral change is typical of the FRET systems and, thus, reasonably ascribed to the facilitated FRET between the coumarin and the styryl dye upon the PhP binding to **4**. On the other hand, the reverse pattern was found for the ATP binding; that is, the peak at 485 nm was intensified and the peak at 569 nm decreased with the addition of ATP (I_{569}/I_{485} changed from 1.1 to 0.72). On the basis of the above-mentioned receptor redistribution induced by the guest-binding, the spectral change is reasonably explained as follows: Before the guest addition, the coumarin-appended receptor **4** predominantly localizes in the bulk aqueous space and the styryl dye **5** is fixed in the hydrophobic nanofiber. Upon the PhP binding, the complexed receptor, **4**/PhP, transfers to the more hydrophobic domain due to the increased hydrophobicity, and as a result, the average

(8) (a) Lottenberg, R.; Christensen, U.; Jackson, C. M.; Coleman, P. L. *Methods Enzymol.* **1981**, *80*, 341−361. (b) Matayoshi, E. D.; Wang, G. T.; Krafft, G. A.; Erickson, J. *Science* **1990**, *247*, 954−958. (c) Oh, E.; Hong, M.-Y.; Lee, D.; Nam, S.-H.; Yoon, H. C.; Kim, H.-S. *J. Am. Chem. Soc.* **2005**, *127*, 3270. (d) Medintz, I. L.; Clapp, A. R.; Mattoussi, H.; Goldman, E. R.; Fisher, B.; Mauro, J. M. *Nat. Mater.* **2003**, *2*, 630.

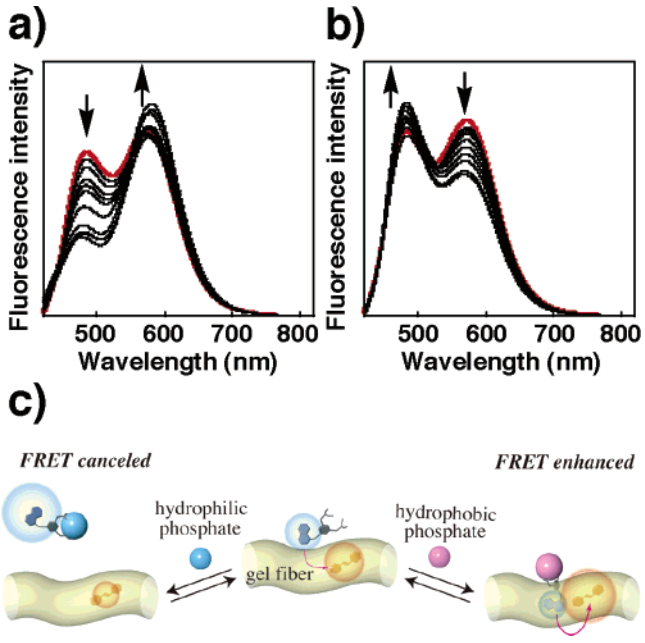

Figure 6. Fluorescence spectral change and fluorescence titration plots of the hydrogel **1** including the coumarin-appended receptor **4** and the styryl dye **5** in the titration of PhP (a) or ATP (b), respectively: [**4**] = 50 μM, [**5**] = 50 μM, and [PhP] or [ATP] = 0−500 μM at λ_{ex} = 393 nm. (c) Illustration of the guest-dependent FRET system using **4** and **5** by the addition of PhP or ATP in the hydrogel matrix.

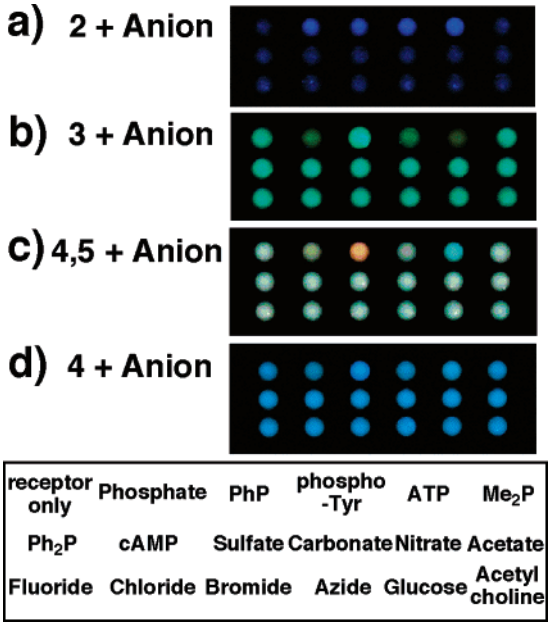

Figure 7. Digital camera photographs of the sensing patterns of semi-wet molecular recognition (MR) chips of the hydrogel **1** containing (a) the bis-Zn/Dpa-anthracene **2** (40 μM), (b) the dansyl-appended receptor **3** (60 μM), (c) the coumarin-appended receptor **4** (50 μM) with the styryl dye **5** (50 μM), and (d) **4** (50 μM) without **5** in the presence of various anions. The spotted position of anions is shown in the bottom of the figure **6**: [anion] = 200 (a), 500 (b), or 600 μM (c,d).

distance between these two fluorophores becomes shorter so as to facilitate the FRET. On the other hand, the receptor **4** complexed with ATP, **4**/ATP, transfers to the more hydrophilic cavity due to the increased hydrophilicity, so that the distance between the two fluorophores becomes longer, which suppresses the FRET. We also confirmed that only the coumarin emission (485 nm) appeared and practically did not change upon the addition of PhP or ATP without the styryl dye (Supporting Information Figure S3). As another control experiment, agarose gel was used for this FRET system, with the result that the emission from **5** did not appear, probably because **5** formed nonfluorescent self-aggregates like a micelle, and the coumarin emission did not change even with the addition of the phosphate derivatives. These results imply that the present supramolecular gel fiber provides a unique hydrophobic microdomain to efficiently incorporate the surfactant-like **5** as the monomeric dispersion to emit the strong fluorescence as a FRET acceptor so as to facilitate the present FRET signal transduction.

For rapid and high-throughput sensing, we next arranged the miniaturized hydrogels on a glass substrate to yield a semi-wet molecular recognition (MR) chip. Figure 7a,b shows photographs of the MR chip containing the PET-type chemosensor **2** and the dansyl-appended receptor **3** in the presence of various anions, respectively. In the case of the chemosensor **2**, it is apparent that the intensified blue fluorescence at the spots including phosphate, PhP, ATP, and phospho-Tyr can be distinguished by the naked eye, whereas a rather weak emission was observed at spots including other anions. In addition to the intensity change, the color change was induced for the environmentally sensitive dansyl-appended receptor **3** embedded in the MR chip. Similar to Figure 7a, the four spots including phosphate, PhP, ATP, and phospho-Tyr can be distinguished by the emission change, but the changing pattern is different from that of chemosensor **2**. That is, an intensified blue emission was observed at the spot containing PhP, whereas a greenish emission was observed at the spot including ATP. The spots containing phosphate or phospho-Tyr emit a slightly green color. Such a color change agrees well with the above-mentioned spectral change, which makes it possible to easily discriminate phosphate derivatives from each other by visual observations.

Figure 7c,d shows photos of the MR chips containing the coumarin-appended receptor **4** with or without the styryl dye **5**, the FRET acceptor. Clearly, the color of the hydrogel changed from purplish to orange at the spot of the PhP addition, or to bluish at the spot of the ATP addition, whereas no distinct color change was observed in the absence of **5**. These photographic images demonstrate that the FRET type of read-out mode may improve the signal discrimination efficiency, compared to the case using the simple environmentally sensitive probe.

Conclusion

In summary, we have demonstrated that a semi-wet supramolecular hydrogel is unique for constructing a novel molecular recognition chip. It was directly observed that the fluorescent receptors can dynamically move from the aqueous cavities to the hydrophobic fibers, or the opposite way, upon guest-binding under the semi-wet conditions provided by the supramolecular hydrogel. On the basis of such a dynamic localization change, the molecular recognition and the fluorescent discrimination toward phosphate derivatives were carried out. The use of the hydrophobic fibrous domain of the supramolecular hydrogel as well as the water-rich hydrophilic cavity rationally produced three distinct signal transduction modes: a PET type, an environmentally sensitive type, and a FRET type of fluorescent signal transduction. By cooperation of the receptor with the supramolecular nanofibers, artificial receptors, which bind phosphate but do not fluorescently sense it, are successfully

converted to fluorescent chemosensors, as shown in the typical examples of receptors **3** and **4**. Thus, the various phosphate derivatives, such as phosphate, phospho-tyrosine, phenyl phosphate, and ATP, can be sensed and discriminated from each other on the basis of the combination of the several parameters yielded by the present MR chip, that is, the fluorescence wavelength shift and ratiometric fluorescence change, as well as the simple fluorescence intensity change. Recently, supramolecular organo- or hydrogels have been actively developed as a new class of self-assembled materials.[9] In contrast to the well-studied structural analysis, novel functions originating from the supramolecular gels have not yet been sufficiently developed. It is expected that the present results will inspire function-directed research into these promising soft materials.

Experimental Section

Generals. Mass spectra were recorded on PB Biosystems Voyager DE-RP MALDI-TOF mass spectrometer. Fluorescence spectra of the hydrogel chips were recorded using an Otsuka Electronics high sensitivity Spectro multichannel photodetector, MCPD-7000. Fluorescence spectra for the aqueous solution were collected on a Hitachi F-4500 instrument. Confocal laser scanning microscopy observation was carried out with a Carl Zeiss LSM 510 device.

Synthesis. The gelator **1**[10] and the chemosensor **2**[3b] were prepared according to the method reported previously by us. The receptors **3** and **4** were prepared as shown in Scheme 1. 3,5-Bis(bromomethyl)-benzyl alcohol was prepared from trimethyl 1,3,5-benzenetricarboxylate following a procedure described in a literature.[11]

3,5-Bis(2,2′-dipicolylaminomethyl)benzyl Alcohol (5). A mixture of 3,5-bis(bromomethyl)benzyl alcohol (570 mg, 1.9 mmol), 2,2′-dipicolylamine (860 mg, 4.3 mmol), and potassium carbonate (1.1 g, 7.9 mmol) in DMF (25 mL) was stirred at room temperature for 50 min under a nitrogen atmosphere, and then ethyl acetate and water were added to the mixture. The organic layer was collected, and the aqueous layer was extracted with ethyl acetate. The initial organic layer and eluant were combined, washed (brine), dried ($MgSO_4$), and filtered. The filtrate was concentrated to dryness, and the residue was purified by column chromatography (SiO_2, dichloromethane/methanol/aqueous ammonia = 100:10:1), affording a yellow oil (870 mg, 84%): ^{1}H NMR (400 MHz, $CDCl_3$) δ 3.68 (s, 4H), 3.79 (s, 8H), 4.68 (s, 2H), 7.05−7.15 (m, 4H), 7.29 (s, 2H), 7.40 (s, 1H), 7.54−7.64 (m, 8H), 8.46−8.51 (m, 4H); FAB-MS obsd 531.3 $[M + H]^+$, calcd 530.3 ($C_{33}H_{34}N_6O$).

3,5-Bis(2,2′-dipicolylaminomethyl)benzylmethylamine (6). A solution of 3,5-bis(2,2′-dipicolylaminomethyl)benzyl alcohol **5** (380 mg, 0.72 mmol) in 47 wt % of aqueous HBr (40 mL) was refluxed for 3 h. The solution was neutralized with aqueous sodium bicarbonate, and the resulting solution was extracted with ethyl acetate. To the organic layer was added 40 wt % of methylamine in methanol (21 mL), and the mixture was stirred at room temperature for 2 h and then concentrated to dryness. The residue was dissolved in ethyl acetate, and the organic layer was washed (water), dried ($MgSO_4$), and concentrated to dryness. The residue was purified by column chromatography (SiO_2, dichloromethane/methanol/aqueous ammonia = 100:10:2), affording a colorless oil (870 mg, 84%): ^{1}H NMR (400 MHz, $CDCl_3$) δ 2.44 (s, 3H), 3.69 (s, 4H), 3.73 (s, 2H), 3.81 (s, 8H), 7.13−7.16 (m, 4H), 7.22 (s, 2H), 7.42 (s, 1H), 7.59−7.65 (m, 8H), 8.52 (d, J = 5.2 Hz, 4H); FAB-MS obsd 534.3 $[M + H]^+$, calcd 543.3 ($C_{34}H_{37}N_7$).

Scheme 1. Synthesis of Bis-DPA−Zn Complexes

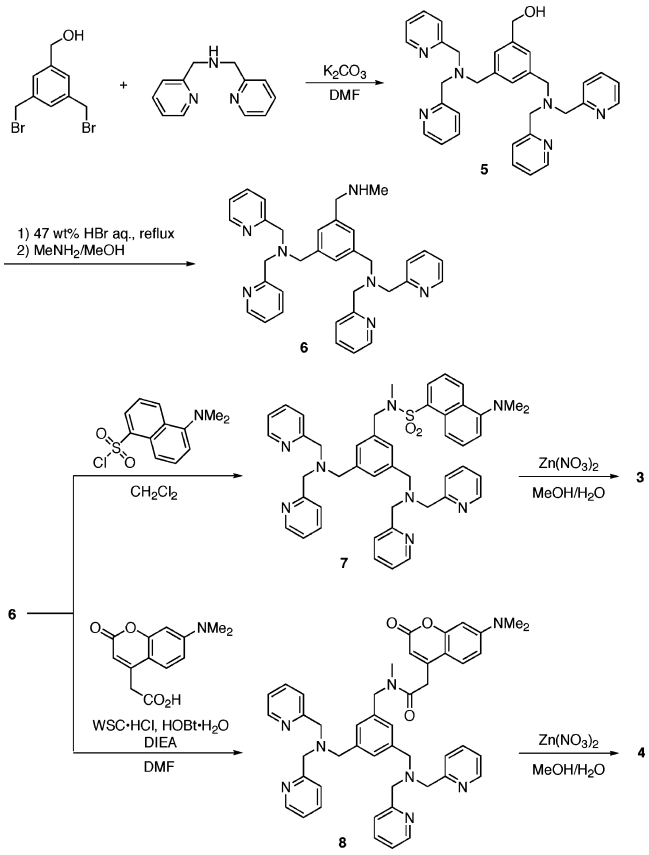

Dansyl-Appended Bis-DPA Compound (7). A solution of 3,5-bis-(2,2′-dipicolylaminomethyl)benzylmethylamine **6** (180 mg, 0.33 mmol) and *N*,*N*′-diisopropylethylamine (DIEA, 90 μL, 0.52 mmol) in dichloromethane (10 mL) was treated with dansyl chloride (110 mg, 0.40 mmol) at 0 °C for 50 min under a nitrogen atmosphere, and then dichloromethane and water were added to the reaction mixture. The organic layer was collected, and the aqueous layer was extracted with dichloromethane. The initial organic layer and eluant were combined, dried ($MgSO_4$), and filtered. The filtrate was concentrated to dryness, and the residue was purified by column chromatography (SiO_2, dichloromethane/methanol/aqueous ammonia = 150:10:2), affording a pale green solid (180 mg, 70%): ^{1}H NMR (400 MHz, $CDCl_3$) δ 2.67 (s, 3H), 2.91 (s, 6H), 3.62 (s, 4H), 3.78 (s, 8H), 7.12−7.15 (m, 4H), 7.20 (s, 1H), 7.22 (s, 2H), 7.39 (s, 1H), 7.53−7.57 (m, 2H), 7.56−7.68 (m, 8H), 8.24 (d, J = 6.8 Hz, 1H), 8.47 (d, J = 8.6 Hz, 1H), 8.51 (d, J = 4.8 Hz, 4H), 8.57 (d, J = 8.6 Hz, 1H); FAB-MS obsd 777.4 $[M + H]^+$, calcd 776.4 ($C_{46}H_{48}N_8O_2S$).

Dansyl-Appended Bis-DPA−Zn Complex (3). To a solution of a dansyl-appended bis-DPA compound **7** (150 mg, 0.19 mmol) in methanol (5 mL) was added 0.05 M zinc(II) nitrate in water (7.6 mL, 0.38 mmol), and the mixture was stirred at room temperature for 30 min in the dark. The mixture was concentrated to dryness, and water was added to the residue. The insoluble material was filtered off and the filtrate was concentrated to dryness, and then the residue was washed with ethyl acetate, affording a pale green solid (200 mg, 92%): ^{1}H NMR (600 MHz, D_2O) δ 2.59 (s, 6H), 3.05 (s, 3H), 3.38 (s, 4H), 3.62

(9) (a) Estroll, L. A.; Hamilton, A. D. *Chem. Rev.* **2004**, *104*, 1202−1217. (b) Kisiday, J.; Jin, M.; Kurz, B.; Hung, H.; Semino, C.; Zhang, S.; Grodzinsky, A. J. *Proc. Natl. Acad. Sci. U.S.A.* **2002**, *99*, 9996−10001. (c) Kobayashi, H.; Friggeri, A.; Koumoto, K.; Amaike, M.; Shinkai, S.; Reinhoudt, D. N. *Org. Lett.* **2002**, *4*, 1423−1426. (d) Jung, J.-H.; John, G.; Masuda, M.; Yoshida, K.; Shinkai, S.; Shimizu, T. *Langmuir* **2001**, *17*, 7229−7232. (e) Menger, F. M.; Caran, K. L. *J. Am. Chem. Soc.* **2000**, *122*, 11679−11691. (f) Maitra, U.; Mukhopadhyay, S.; Sarkar, A.; Rao, P.; Indi, S. S. *Angew. Chem., Int. Ed.* **2001**, *40*, 2281−2283. (g) Estroff, L. A.; Hamilton, A. D. *Angew. Chem., Int. Ed.* **2000**, *39*, 3447−3449. (h) Bhattacharya, S.; Acharya, S. N. G. *Chem. Mater.* **1999**, *11*, 3504−3511. (i) Oda, R.; Huc, I.; Candau, S. J. *Angew. Chem., Int. Ed.* **1998**, *37*, 2689−2691. (j) Makarevic, J.; Jokic, M.; Peric, B.; Tomisic, V.; Kojic-Prodic, B.; Zinic, M. *Chem.−Eur. J.* **2001**, *7*, 3328−3341. (k) Petka, W. A.; Harden, J. L.; McGrath, K. P.; Wirtz, D.; Tirrell, D. A. *Science* **1998**, *281*, 389−392.
(10) Kiyonaka, S.; Zhou, S.-L.; Hamachi, I. *Supramol. Chem.* **2003**, *15*, 521−528.
(11) Díez-Barra, E.; García-Martínez, J. C.; del Rey, R.; Rldríguez-López, J.; Sánchez-Verdú, P.; Tejada, J. *J. Org. Chem.* **2001**, *66*, 5664.

(d, J = 15.8 Hz, 4H), 3.82 (d, J = 15.8 Hz, 4H), 4.41 (br s, 2H), 6.60 (br s, 1H), 6.80 (br s, 2H), 7.15 (m, 1H), 7.22 (d, J = 7.5 Hz, 4H), 7.38 (br s, 2H), 7.51 (br s, 4H), 7.87−7.94 (m, 5H), 8.05 (d, J = 8.6 Hz, 1H), 8.22 (d, J = 8.6 Hz, 1H), 8.62 (br s, 4H); FAB-MS obsd 1094.3 $[M - NO_3]^+$, calcd 1155.8 ($C_{46}H_{48}N_8O_2S{\cdot}2Zn{\cdot}4NO_3$). Anal. Calcd for $C_{46}H_{48}N_8O_2S{\cdot}2Zn{\cdot}4NO_3{\cdot}2H_2O$: C, 46.36; H, 4.40; N, 14.10. Found: C, 46.13; H, 4.29; N, 14.10.

Coumarin-Appended Bis-DPA Compound (8). A solution containing 3,5-bis(2,2′-dipicolylaminomethyl)benzylmethylamine **6** (170 mg, 0.31 mmol), dimethylaminocoumarin-4-acetic acid (100 mg, 0.40 mmol), 1-hydoxybenzotriazole monohydrate (HOBt·H_2O, 62 mg, 0.40 mmol), 1-ethyl-3-(3-dimethylaminopropyl)carbodiimide hydrochloride (WSC·HCl, 78 mg, 0.40 mmol), and DIEA (160 μL, 0.93 mmol) was stirred at room temperature for 24 h, and then ethyl acetate and water were added to the reaction mixture. The organic layer was collected, and the aqueous layer was extracted with ethyl acetate. The initial organic layer and eluant were combined, washed (aqueous sodium bicarbonate followed by brine), dried ($MgSO_4$), and filtered. The filtrate was concentrated to dryness, and the residue was purified by column chromatography (SiO_2, dichloromethane/methanol/aqueous ammonia = 100:10:1 to 300:10:3), affording a yellow amorphous solid (142 mg, 59%): ^{1}H NMR (400 MHz, $CDCl_3$) δ 2.93, 3.02 (s, 3H), 3.00, 3.03 (s, 6H), 3.67, 3.69 (s, 4H), 3.72, 3.77 (s, 2H), 3.79, 3.80 (s, 8H), 4.52, 4.60 (s, 2H), 5.94, 5.98 (s, 1H), 6.42−6.56 (m, 2H), 7.10−7.17 (m, 6H), 7.38−7.46 (m, 2H), 7.53−7.66 (m, 8H), 8.49−8.52 (m, 4H). The compound was found to be a conformational mixture of the cis and trans isomers along the amide bond in the NMR time scale: FAB-MS obsd 773.4 $[M + H]^+$, calcd 772.4 ($C_{47}H_{48}N_8O_3$).

Coumarin-Appended Bis-DPA−Zn Complex (4). Following the procedure described for the dansyl-appended bis-DPA Zn complex **3**, the zinc complex **4** was prepared as a yellow powder (87 mg, 66%): FAB-MS obsd 1086.3 $[M - NO_3]^+$, calcd 1148.2 ($C_{47}H_{48}N_8O_3{\cdot}2Zn{\cdot}4NO_3$). Anal. Calcd for $C_{46}H_{48}N_8O_2S{\cdot}2Zn{\cdot}4NO_3{\cdot}H_2O$: C, 48.26; H, 4.31; N, 14.37. Found: C, 48.16; H, 4.31; N, 14.59.

Preparation of a Supramolecular Gel Array. The gel array was prepared according to a slight modification of the method reported previously by us.[4f] A suspension of gelator **1** (1 mg) in 50 mM HEPES buffer (pH 7.2, 200 μL) was heated to form a homogeneous solution. A 10 μL portion of the hot solution was spotted on the glass plate and incubated to complete gelation in a sealed box with high humidity at room temperature for 30 min. One microliter of chemosensor or analyte solution (in 50 mM HEPES buffer, pH 7.2) was dropped onto each resultant hydrogel spot, respectively, by using a micropipet.

Fluorescence Measurement of Molecular Recognition Events in the Hydrogel. The fluorescence spectral change of the hydrogel containing a chemosensor was traced by the multichannel photodetector (MCPD) at room temperature. The photographic images of the resulting MR chip were collected by using a digital camera equipped with a cut-off filter (<420 nm) under UV irradiation (λ_{ex} = 365 nm, using a handy lamp).

CLSM Observation. A hydrogel spot was prepared on a dish for CLSM observation by the procedure described above. An anlalyte solution (1 μL) was dropped onto the hydrogel spot, and then the change of the image during the molecular recognition process was observed by CLSM.

Acknowledgment. Shun-ichi Tamaru is a JSPS postdoctoral fellow.

Supporting Information Available: Fluorescence spectra and the chemical structure of octadecyl rhodamine B. This material is available free of charge via the Internet at http://pubs.acs.org.

JA052838Y